Published in final edited form as:
Neuroscience. 2010 February 17; 165(4): 1447. doi:10.1016/j.neuroscience.2009.11.032.

Calcium-induced calcium release contributes to synaptic release from mouse rod photoreceptors

N. Babai[1], **C. W. Morgans**[2], and **WB. Thoreson**[1]

[1]Department of Ophthalmology and Visual Sciences, University of Nebraska Medical Center, Omaha, NE

[2]Casey Eye Institute, Oregon Health & Science University, Portland, OR.

Abstract

We tested whether calcium-induced calcium release (CICR) contributes to synaptic release from rods in mammalian retina. Electron micrographs and immunofluorescent double labeling for the sarco/endoplasmic reticulum Ca^{2+}-ATPase (SERCA2) and synaptic ribbon protein, ribeye, showed a close association between ER and synaptic ribbons in mouse rod terminals. Stimulating CICR with 10 μM ryanodine evoked Ca^{2+} increases in rod terminals from mouse retinal slices visualized using confocal microscopy with the Ca^{2+}-sensitive dye, Fluo-4. Ryanodine also stimulated membrane depolarization of individual mouse rods. Inhibiting CICR with a high concentration of ryanodine (100 μM) reduced the ERG b-wave but not a-wave consistent with inhibition of synaptic transmission from rods. Ryanodine (100 μM) also inhibited light-evoked voltage responses of individual rod bipolar cells (RBCs) and presumptive horizontal cells recorded with perforated patch recording techniques. A presynaptic site of action for ryanodine's effects is further indicated by the finding that ryanodine (100 μM) did not alter currents evoked in voltage-clamped RBCs by puffing the mGluR6 antagonist, (RS)-α-cyclopropyl-4-phosphonophenylglycine (CPPG), onto bipolar cell dendrites in the presence of the mGluR6 agonist L-(+)-2-amino-4-phosphonobutyric acid (L-AP4). Ryanodine (100 μM) also inhibited glutamatergic outward currents in RBCs evoked by electrical stimulation of rods using electrodes placed in the outer segment layer. Together, these results indicate that, like amphibian retina, CICR contributes to synaptic release from mammalian (mouse) rods. By boosting synaptic release in darkness, CICR may improve the detection of small luminance changes by post-synaptic neurons.

Keywords

Ca-induced Ca^{2+}; release; ryanodine; outer retina; synaptic transmission

INTRODUCTION

Release of the neurotransmitter, L-glutamate, from rod photoreceptors is controlled by the influx of Ca^{2+} through L-type Ca^{2+} channels clustered the near the synaptic ribbon in rod

Address for Correspondence: Wallace B. Thoreson Department of Ophthalmology and Visual Sciences University of Nebraska Medical Center 4050 Durham Research Center Omaha, NE 68198-5840 Phone: 402 559 2019 Fax: 402 559 5368 wbthores@unmc.edu.

terminals (Heidelberger *et al*, 2005). In amphibian rods, this Ca^{2+} influx can trigger release of Ca^{2+} from intracellular stores to amplify synaptic exocytosis (Krizaj *et al*. 1999; Suryanarayanan & Slaughter, 2006; Cadetti *et al*. 2006). Calcium-induced calcium release (CICR) is particularly prominent with maintained depolarization and boosts synaptic release when rods are maintained at relatively depolarized resting membrane potentials in darkness of ca. −40 mV (Suryanarayanan & Slaughter, 2006; Cadetti *et al*. 2006). CICR has also been shown to contribute to synaptic release at other CNS synapses (Bouchard *et al*. 2003; Collin *et al*. 2005) including ribbon synapses of hair cells (Lelli *et al*. 2003).

CICR is mediated by the activation of ryanodine receptors located on the endoplasmic reticulum. Retina possesses all three types of ryanodine receptors (RyR1, RyR2, and RyR3) but the predominant subtype is a retina-specific variant of RyR2 (Shoshan-Barmatz *et al*. 2005, 2007). Pan-RyR antibodies label the outer plexiform layer (OPL) (Shoshan-Barmatz *et al*. 2005, 2007) and ultrastructural studies of frog rods indicate the presence of smooth endoplasmic reticulum (ER) that can accumulate calcium ions in the synaptic terminals (Ungar *et al*. 1981; Mercurio & Holtzman, 1982).

In the present study, we tested whether, like amphibian rods, CICR contributes to the regulation of intraterminal Ca^{2+} levels in mouse rods. There are both similarities and differences between the synaptic terminals of amphibian and mammalian rods. For example, synaptic ribbons of amphibian and mammalian rods are similar in size and appearance, but amphibian rods have 5-7 ribbons whereas mammalian rods possess only 1-2 ribbons (Townes-Anderson et al, 1985; Migdale et al, 2003). The amplitude and voltage dependent properties of I_{Ca} are also similar in salamander and mouse rods (Babai and Thoreson, 2008), but salamander rod I_{Ca} exhibits Ca^{2+} dependent inactivation whereas CaV1.4, the principal I_{Ca} subtype in mammalian rods, does not (Rabl & Thoreson, 2002; Koschak et al, 2003; McRory et al, 2004; Baumann et al, 2004). Our results indicate that, much like amphibian rods, ryanodine receptors in mouse rods mediate a release of Ca^{2+} from ER close to the ribbon that can enhance synaptic release.

EXPERIMENTAL PROCEDURES

Mouse retinal slices

Mice (*Mus musculus*, C57BL6J, Jackson Laboratory, Bar Harbor, ME) were sacrificed by CO_2 inhalation. One eye was then rapidly enucleated and the anterior segment of the eye removed.

For eyecup preparations, we used a superfusion chamber modeled on that of Newman and Bartosch (1999) in which the eyecup is everted over a small plastic dome and held in place by the top half of the chamber. A circular opening in the top half of the chamber exposed the vitreal surface of the eyecup for superfusion and recording. Intraretinal ERGs were recorded from eyecup preparations using a saline-filled micropipette (10-15 MΩ) referenced to an Ag/AgCl pellet in the base of the chamber. ERGs were low pass filtered at 1 kHz. In some cases, they were also high pass filtered at 0.1 Hz. The amplitude of the b-wave was measured from the trough of the a-wave to the peak of the b-wave.

For retinal slice preparation, mouse eyecup was placed vitreal side down on a piece of filter paper (2 × 5 mm, Type AAWP, 0.8 μm pores, Millipore, Bedford, MA, USA). To maintain light responses, slices were prepared under infrared illumination using night vision goggles (Nitemate NAV3, Litton Industries, Tempe, AZ). After adhering to the filter paper, the retina was isolated from the sclera, carefully cutting the optic nerve attachment. Cold superfusate was then added to the chamber and retinal slices (125 μm) were cut with a razor blade tissue chopper (Stoelting, Wood Dale, IL, USA). Slices were positioned in the recording chamber for viewing of the retinal layers on an upright fixed stage microscope (Nikon E600 FN, Japan)

using a long-working distance water immersion objective (60X, 1.0 NA). Slices were superfused at 32-35 deg C at a rate of ~1 ml/min with a solution containing (in mM): 120 NaCl, 22.6 $NaHCO_3$, 3 KCl, 0.5 KH_2PO_4, 2 $CaCl_2$, 0.5 $MgSO_4$, 6 glucose. The superfusate was bubbled continuously with 95% O_2 and 5% CO_2.

Electrophysiology

Whole cell recordings were obtained using 10-15 MΩ patch electrodes fabricated from borosilicate glass (1.2 mm O.D., 0.95 mm I.D., with internal filament, World Precision Instruments, Sarasota, FL) on a PP-830 micropipette puller (Narishige USA, East Meadow, NY).

For whole cell voltage clamp recordings from rod bipolar cells (RBCs), we used a pipette solution containing (in mM): 125 CsGluconate, 10 TEACl, 10 HEPES, 3 EGTA, 1 ATP, 0.5 GTP, 3 $MgCl_2$, 1 $CaCl_2$ (pH 7.2). RBCs were identified by their large cell bodies in the distal inner nuclear layer, confirmed in some cases by fluorescent staining with the dye Lucifer Yellow (2 mg/ml). RBCs were clamped at a holding potential of −50 mV. For current clamp recordings from rods and second order neurons, we used gramicidin (5 μg/ml) or amphotericin B (25 μM) as a perforating agent along with a pipette solution containing (in mM): KCH_3SO_4, 98; KCl, 44; NaCl, 3; HEPES, 5; EGTA, 3 mM; $MgCl_2$, 3; $CaCl_2$, 1; glucose, 2; Mg-ATP, 1; GTP, 1 (pH 7.2). Electrophysiological data was recorded using an Axopatch 200B or Multiclamp amplifer (Axon Instruments, Molecular Devices, Sunnyvale, CA) along with a Digidata 1200 or 1322 interface and PClamp 9.2 software (Axon Instruments).

Light stimuli were generated using a 50 W halogen lamp focused onto a fiber optic reflected through a beam splitter into the microscope condenser. We used a white light stimulus which contains photons that are ineffective in stimulating the mouse retina. From quantitative comparisons of ERG responses to flashes of white and 480 nm light, we calculated the effective intensity of the white light stimulus in units of 480 nm equivalent photons s^{-1} μm^{-2} (Burkhardt et al, 1988). We then measured the intensity of the 480 nm light using a laser power meter (Metrologic, Blackwood, NJ). Half-maximal responses to 0.5 s steps of lights were obtained at an intensity of 500 ± 50 (N=3) 480 nm equivalent photons s^{-1} μm^{-2} consistent with rod-dominated inputs (Nikonov et al, 2006; Nakatani et al, 1991). For most experiments, we used white light stimuli ranging from 1.3×10^3 −1.8×10^4 480 nm equivalent photons s^{-1} μm^{-2}. This is below the intensity required to evoke half maximal responses to steps of light in mouse M cones (e.g., 2.5×10^5 photons s^{-1} μm^{-2} at 501 nm; Nikonov et al, 2006) but it is possible that M cone inputs may have contributed to some of the observed responses. The light source generated more than 1.5 log units less energy at 380 nm so S cone inputs are less likely.

Ca^{2+} Imaging

Mouse retinal slices were incubated with 10 μM Fluo4-AM dissolved in 0.5 ml Hibernate-A solution (Brain Bits LLC, Sringfield, IL) for ~1 hr. at room temperature in darkness. Confocal images were acquired using a laser confocal scanhead (Perkin Elmer Ultraview LCI) equipped with a cooled CCD camera (Orca ER) and mounted to a fixed stage upright microscope (Nikon E600 FN). Excitation and emission were controlled by a Sutter Lambda 10-2 filter wheel and controller. Images were acquired and analyzed using UltraView Imaging Suite software. The objective (60X; 1.0 NA) was controlled with a Z-axis controller (E662 Physik Instrumente, Germany) to acquire a series of slices (1 μm steps) at each time point. The duration of individual frames ranged from 100-200 ms and each z-stack of images was acquired at 10 s intervals. For illustration, contrast and brightness were enhanced using Adobe Photoshop.

Immunohistochemistry

Freshly dissected mouse eyes were hemisected and the posterior eyecups fixed by immersion in 4% (w/v) paraformaldehyde in phosphate-buffered saline (PBS; pH 7.4) for 10-20 minutes at 4°C. The eyecups were then cryoprotected in graded sucrose-PBS (10%, 20% and 30% w/v). The eyecups were embedded in OCT (Tissue-Tek, Elkhart, IN), quick frozen by submersion in an isopentane/dry ice bath. Vertical sections were cut on a cryostat at 16 μm thickness, mounted onto Superfrost/Plus slides (Fisher Scientific, Pittsburgh, PA), and stored frozen at −80°C. After thawing, sections were blocked by incubation for 60 min at room temperature in Antibody Incubation Solution (AIS) (0.5% Triton X-100, 3% serum, 0.05% NaN_3 in PBS). Sections were then incubated with rabbit anti-SERCA2 antibody (1:200 – 1:400; Abcam Inc, Cambridge, MA) in combination with mouse anti-CtBP2 (ribeye, 1:5000; BD Biosciences, USA) diluted in AIS for 2 hr at room temperature. Following three washes in PBS, the tissue was incubated for 1 hr at room temperature with anti-rabbit IgG conjugated to Alexa Fluor 594 (1:1000; Invitrogen, Carlsbad, CA) in combination with anti-mouse-488 (1:1000; Invitrogen), then washed again in PBS. After three final washes in PBS, sections were coverslipped in Aqua-Mount mounting medium (Lerner Laboratories, Pittsburgh PA), and images acquired with an Olympus FluoView FV1000 confocal microscope using a 60X/1.42 oil immersion objective.

Electron microscopy

Eyecups, prepared as described above, were fixed in 2% glutaraldehyde/0.1 M cacodylate buffer for 2 hours, then osmicated in 2% OsO4 in 0.1 M phosphate buffer, pH 7.4, for 1 hour, and dehydrated through an ethanol series and propylene oxide. Following an overnight incubation in 1:1 propylene oxide:Embed 812 (Electron Microscopy Sciences, Hatfield, PA), the samples were embedded and cured in Embed 812 (Ted Pella, Redding, CA). Sections of 75 nm were cut with a Leica ultramicrotome, mounted onto 400 thin-bar copper grids, and contrasted with uranyl acetate and lead citrate before being viewed on a FEI Tecnai 12 microscope. Images were captured digitally by using a Hamamatsu camera. Contrast and brightness were enhanced using Adobe Photoshop.

Chemicals

Ryanodine was generously provided by Dr. Keshore Bidasee, University of Nebraska Medical Center. Unless otherwise specified, other chemicals were obtained from Sigma/Aldrich (St. Louis, MO).

Statistics

The criterion for statistical significance was chosen to be $p < 0.05$ and evaluated using Student's T-test and GraphPad Prism 4.0. Variability is reported as ± SEM.

RESULTS

For CICR to contribute to release from mouse rods, ER should be located in rod terminals close to the synaptic ribbons that mediate release. Immunofluorescent double labeling for the ER protein, SERCA2, and the ribbon protein, ribeye, show a close association between the ER and synaptic ribbons in rod terminals (Fig. 1A). The SERCA2 antibody labels irregularly shaped structures within the OPL that coincide with synaptic ribbons in rod terminals; also labeled were dense plaques that could be double labeled with peanut agglutinin indicating association with cone terminals (not shown). The close association between rod synaptic ribbons and putative ER was confirmed by examining rod terminals using electron microscopy. As shown in Fig. 1B, intracellular membranes characteristic of smooth ER are clearly visible within rod terminals in close proximity to the active zone. The distance from the base of the synaptic

ribbon to the nearest ER-like structure in twenty rod terminals averaged 565 ± 298 nm. ER-like profiles were also observed in cone terminals, but not bipolar cell terminals (not shown).

At low concentrations ryanodine acts as an agonist to stimulate release of calcium from intracellular stores (Rousseau *et al*. 1987; Pessah & Zimanyi, 1991). We tested for the presence of CICR in rods by determining whether low concentrations of ryanodine stimulated intracellular Ca^{2+} increases in individual rods. We loaded retinal slices with the calcium-sensitive dye, Fluo4-AM, and visualized individual cell bodies and rod terminals by confocal microscopy. As shown in Fig. 2, bath application of 10 μM ryanodine stimulated calcium increases in mouse rod somas. Fig. 2A-C show Fluo4-loaded retinal slices before, during, and after bath application of ryanodine. Each image shows a single confocal section. Fig. 2D graphs the fluorescence changes measured in 19 different rod somas from the same retinal slice and Fig. 2E shows the average of these responses. Large Ca^{2+} increases could be observed in many cells, typically preceded by a smaller gradual increase. Large Ca^{2+} increases appeared in some cells soon after ryanodine application but occurred much later in other cells. Large increases in Ca^{2+} sometimes occurred even after beginning wash out of ryanodine from the chamber, suggesting a slow recovery from ryanodine. To determine the frequency of observed Ca^{2+} increases, we examined responses from every cell body within rectangular regions from single confocal sections in 16 different experiments. Within rectangular regions encompassing 24-43 somas (mean = 33), 84 ± 1.2% (N=16 slices) of adjacent cell bodies exhibited a Ca^{2+} increase after ryanodine application. We observed a smaller percentage of responsive cells in confocal sections near the surface of the retinal slice, presumably because many of these cells were damaged by slicing. These results indicate that, like amphibian photoreceptors (Krizaj *et al*. 1999; 2003; Cadetti *et al*. 2006), activation of CICR by ryanodine can stimulate Ca^{2+} increases in mammalian rods.

In contrast with the slow onset and variable timing of large Ca^{2+} changes produced by ryanodine, depolarizing rods to ~−35 mV by bath application of 30 mM K^+ (Babai & Thoreson, 2009) caused rapid Ca^{2+} increases that occurred at nearly the same time in every cell and recovered rapidly after washout (Fig. 3). The ~30 s delay between the start of high K^+ application and appearance of the first Ca^{2+} response reflects the time required for test solution to reach the chamber.

In addition to somatic increases, ryanodine (10 μM) also stimulated Ca^{2+} increases in rod terminals in the OPL (Fig. 4). Fig. 4A-C shows single confocal sections of the OPL loaded with Fluo4-AM before, during, and after bath application of ryanodine (10 μM). Fig. 4D plots the change in intraterminal Ca^{2+} measured every 10 s from 12 terminals in this section of the; Fig. 4E shows the average response from those terminals. It is possible that some of the fluorescent spots in the OPL were cone terminals, but most were probably rod terminals since cone terminals are larger, fewer in number, and closer to the INL than rod terminals (Babai & Thoreson, 2009). In single confocal sections from each of 16 different retinal slice preparations, we found at least 15 ± 2 terminals/section (range 9-38) that exhibited Ca^{2+} increases after ryanodine application. The finding that ryanodine is capable of stimulating Ca^{2+} increases in many rod terminals supports the hypothesis that CICR may regulate Ca^{2+} levels at the rod synapse.

As a further test of whether activation of CICR can influence the activity of individual rods, we recorded the membrane potential from rods using gramicidin-perforated patch recording techniques. Intracellular Ca^{2+} increases can stimulate calcium-activated chloride channels in photoreceptors (Barnes & Hille, 1989) and this can cause membrane depolarization because of the relatively depolarized value of E_{Cl} in rods (Thoreson *et al*. 2002). We therefore hypothesized that ryanodine-induced Ca^{2+} increases should depolarize mouse rods. In control conditions, the rod resting potential averaged −46.7 ± 3.32 mV (N = 7). Addition of ryanodine

(10 μM) depolarized rods by an average of 13.3 ± 3.96 mV (N = 7, P = 0.015). In two cells, a modest initial depolarization was followed by an abrupt depolarization exceeding 20 mV in amplitude that was maintained for many seconds (Fig. 5). If we omit the amplitude of these large depolarizing responses from membrane potential measurements, then the ryanodine-evoked depolarization averaged 7.2 ± 2.76 mV (N = 7, P = 0.007). The waveform of the large depolarizing responses observed in these two cells was similar to prolonged depolarizing responses observed in rods from other species that arise from the activation of calcium and calcium-activated chloride channels (Burkhardt *et al*. 1991; Thoreson & Burkhardt, 1991; Barnes & Deschenes, 1992). It is possible that these large depolarizing responses were responsible for the large, abrupt somatic Ca^{2+} increases observed with Ca^{2+} imaging. The finding that low concentrations of ryanodine stimulated membrane depolarization in rods provides further evidence that activation of CICR can have presynaptic effects on individual rod photoreceptors in the mouse retina.

The ERG b-wave arises from light responses of ON bipolar cells whereas the a-wave reflects photoreceptor responses (Stockton & Slaughter, 1989; Robson & Frishman, 1998). The scotopic b-wave in mouse retina largely reflects RBC responses and can thus be used to assess synaptic transmission from rods to RBCs (Sharma *et al*. 2005). Whereas low concentrations of ryanodine activate CICR, high concentrations of ryanodine inhibit CICR (Bouchard *et al*. 2003). As shown in Fig. 6A, blocking CICR with a high concentration of ryanodine (100 μM) significantly inhibited the ERG b-wave evoked by 0.5 s light flash (−37.3 ± 2.25%, N = 7, P = 0.0081) but did not significantly reduce the accompanying a-wave (−13.9 ± 6.79%, N = 4, P = 0.13). Light flashes were not always bright enough to generate a measurable a-wave preceding the b-wave. The b-wave recovered after washout of ryanodine (Fig. 6A). The ability to obtain recovery after washout of ryanodine is consistent with the finding that ryanodine dissociates more rapidly from the retina-specific RyR2 variant than other RyR subtypes (Shoshan-Barmatz *et al*. 2005). To isolate the a-wave, we blocked the b-wave with L-AP4 (10 μM). Ryanodine (100 μM) also did not significantly inhibit the AP4-isolated a-wave evoked by 100 ms light flashes (−7.8 ± 7.5%; P=0.38, N=6; Fig. 6B). To block possible inner retinal effects on the b-wave (Bui & Fortune, 2004; Robson & Frishman, 1998), we also tested ryanodine (100 μM) in the presence of the NMDA and non-NMDA antagonists, MK801 (100 μM) and NBQX (10 μM). Similar to effects obtained without these antagonists, ryanodine reduced the b-wave by 29.6 ± 3.7% (N=9, P<0.0001). The finding that a high concentration of ryanodine significantly inhibited the ERG b-wave but not the a-wave indicates that blocking CICR inhibits ON bipolar cell light responses but has little effect on photoreceptor light responses.

By stimulating CICR, caffeine can empty intracellular stores of Ca^{2+} in photoreceptors (Krizaj *et al*. 2003). Consistent with a role for CICR in release, treatment of the retina with caffeine (10 mM) significantly reduced the b-wave (−63.2 ± 7.50%, N = 5, P = 0.0011). However, caffeine also significantly reduced the a-wave (−70.9 ± 6.82%, N = 4, P = 0.0019) consistent with previous reports that caffeine inhibits photoreceptor light responses by virtue of its inhibitory effect on phosphodiesterase activity (Capovilla *et al*. 1982; Schneider & Zrenner, 1986). Because of caffeine effects on photoreceptor light responses, we used ryanodine to manipulate CICR in most of our experiments.

We then examined effects of ryanodine (100 μM) on light-evoked voltage responses of individual second order neurons recorded from retinal slices using perforated patch recording techniques. We recorded depolarizing light responses from RBCs (Fig. 7A) and hyperpolarizing light responses from second order neurons that were likely horizontal cells (Fig. 7B). As illustrated in Fig. 8, depolarizing light responses of RBCs and hyperpolarizing light responses of presumptive horizontal cells were both significantly inhibited by bath application of ryanodine (100 μ; RBCs: −26.9± 3.5%, N = 6, P = 0.0006; presumptive

horizontal cells: −46.2± 5.2%, N = 7, P = 0.0001). Inhibition of light responses in the combined sample averaged 32 ± 3.9%, similar to inhibition of the ERG b-wave by ryanodine. Inhibition of the initial peak of the light response immediately after the light flash did not differ significantly from inhibition of the response measured just prior to light offset (P=0.96). Light responses could recover after sufficient washout of ryanodine (Fig. 7). The most parsimonious explanation for the finding that ryanodine inhibited responses of RBCs, whose light responses are mediated by mGluR6 receptors and horizontal (or OFF bipolar) cells whose light responses are mediated by AMPA/KA receptors (reviewed by Thoreson & Witkovsky, 1999) is that ryanodine acts presynaptically to reduce glutamate release from rods. Consistent with a reduction in glutamate release from rods, the membrane potentials of RBCs depolarized by +4.3 ± 0.5mV (P = 0.008, N = 8) and presumptive horizontal cells hyperpolarized by −4.7± 0.67 mV (P = 0.03, N = 6) following ryanodine application.

As an additional test of whether the inhibition of RBC responses by 100 μM ryanodine was presynaptic in origin, we used techniques developed by Nawy (2004) to simulate post-synaptic effects of light responses in voltage-clamped RBCs by puffing an mGluR6 antagonist, CPPG (600 μM), into the OPL while continuously perfusing L-AP4 (4 μM). By antagonizing the L-AP4-evoked outward current, CPPG caused an inward current in RBCs voltage clamped at −50 mV (Fig. 8). CPPG-evoked inward currents exhibited a reversal potential near 0 mV (N = 2) as expected for mGluR6-gated cation channels. However, unlike the true light response, the CPPG-induced inward current was not significantly inhibited by ryanodine (Fig. 8; +1.2 ± 4.7 %, P = 0.91, N = 14) consistent with other evidence that the inhibitory effects of ryanodine on the RBC light response are predominantly pre-synaptic in origin.

Consistent with the minimal effects of ryanodine on the ERG a-wave, Suryanaryan and Slaughter (2006) found that ryanodine had no effect on rod light responses. However, Cadetti et al (2006) reported a small but significant inhibitory effect of ryanodine on rod responses. To bypass phototransduction altogether, we recorded from voltage-clamped RBCs and stimulated synaptic release from rods by injecting extracellular current into the outer segment layer (Hasegawa *et al*. 2006). Extracellular current injection had direct effects on RBCs resulting in a net inward current (Fig. 9) but superimposed on this direct inward current was an outward, synaptically-mediated current that could be revealed by blocking mGluR6 with bath-applied CPPG (600 μM, Fig. 9A) or saturating mGluR6 with L-AP4 (4 μM, not shown). The glutamatergic outward current isolated by subtracting currents evoked in the presence of CPPG from control currents (Fig. 9B) averaged +11.4 ± 3.9 pA (N=6, P=0.04). The L-AP4-sensitive current isolated in the same way averaged +29.5 ± 9.6 pA (N=6, P=0.03). Like L-AP4 and CPPG, ryanodine (100 μM, N = 9) reduced an outward current during current injection in the outer segment layer resulting in a larger net inward current (Fig. 9C). The ryanodine-sensitive current, revealed by subtracting the control trace from the trace obtained in ryanodine, averaged +5.9 ± 2.0 pA (P = 0.02, Fig. 9D). This experiment provides further evidence that 100 μM ryanodine inhibits synaptic glutamate release from rods.

DISCUSSION

In salamander retina, CICR boosts synaptic release from rod terminals by amplifying the effects of calcium entering through voltage-gated L-type Ca^{2+} channels (Krizaj *et al*. 1999; Suryanarayanan & Slaughter, 2006; Cadetti *et al*. 2006). The present study shows that CICR can also enhance synaptic release from rods in mouse retina. Consistent with the presence of CICR in mammalian rods, Shoshan-Barmatz *et al*. (2005, 2007) found that ryanodine receptor antibodies label the OPL of mammalian retina. Our results extend these findings by showing that immunofluorescent labeling for the endoplasmic reticulum protein, SERCA2, co-localizes with rod synaptic ribbons showing the presence of calcium stores near the synaptic release site. Electron micrographs also revealed intracellular membranes characteristic of endoplasmic

reticulum within ~600 nm of the ribbon. Physiological experiments showed that activating ryanodine receptors with a low concentration of ryanodine stimulated Ca^{2+} increases in the terminals and cell bodies of mouse rods. Application of 10 μM ryanodine also caused rods to depolarize. Thus, consistent with results from amphibian retina (Krizaj *et al*. 1999, 2003), RyR receptors in somas and terminals of mammalian rods appear capable of stimulating CICR from intracellular stores in the endoplasmic reticulum.

CICR can activate Ca^{2+}-activated Cl^- channels in photoreceptors (Barnes & Hille, 1989) and activation of these channels would be expected to cause membrane depolarization because E_{Cl} in rods is ca. −20 mV (Thoreson *et al*. 2002), more positive than the resting potential of ca. −45 mV. The finding that ryanodine stimulated membrane depolarization of mouse rods is consistent with stimulation of Ca^{2+}-activated Cl^- channels by CICR in rods. In two rods, we observed large, prolonged depolarizing responses with waveforms similar to prolonged depolarizing responses found in rods and cones of other species (Burkhardt *et al.* 1988, 1991; Thoreson & Burkhardt, 1991; Barnes & Deschenes, 1992). These earlier studies showed that prolonged depolarizing responses begin when an initial small depolarization (e.g., due to activation of Ca^{2+}-activated Cl^- channels by CICR) stimulates the regenerative activation of voltage-gated Ca^{2+} channels. Ca^{2+} influx through open Ca^{2+} channels then stimulates additional Ca^{2+}-activated Cl^- channels and the depolarizing influence of these channels helps to extend the plateau of the Ca^{2+} action potential (Burkhardt et al, 1988; Thoreson & Burkhardt, 1991; Barnes & Deschenes, 1992). The abrupt increase in Ca^{2+} influx accompanying regenerative, prolonged depolarizing responses could account for the large abrupt Ca^{2+} increases observed at varying times after application of ryanodine.

Blocking CICR with a high concentration (100 μM) of ryanodine inhibited the ERG b-wave and light responses of individual RBCs but did not significantly reduce the ERG a-wave suggesting that ryanodine inhibits synaptic transmission from rods to RBCs but has little or no effect on rod light responses. The absence of a significant effect of ryanodine on rod light responses is consistent with findings by Suryanarayanan & Slaughter (2006) although Cadetti *et al*. (2006) reported a small reversible inhibition of light responses. Bypassing light stimulation altogether, we found that ryanodine also inhibited outward glutamatergic currents evoked by electrical stimulation of rods, similar to effects produced by blocking mGluR6 receptors with CPPG or L-AP4. Inhibitory effects of ryanodine on RBC responses were not due to post-synaptic actions at mGluR6 receptors since ryanodine did not inhibit receptor-mediated currents evoked by puffing CPPG into the outer plexiform layer in the presence of L-AP4. Furthermore, hyperpolarizing light responses of presumptive horizontal cells were also inhibited by ryanodine. From these results, we conclude that, like amphibian retina, CICR contributes to synaptic release from rods in mammalian retina. It is possible that cones may have contributed to light responses in some of these experiments and this raises the possibility that CICR may also contribute to the regulation of synaptic release from cones. However, there is little evidence for a contribution of CICR to release from cones in the amphibian retina (Krizaj et al 2003; Thoreson 2007).

CICR works in concert with other mechanisms including voltage-gated and store-operated Ca^{2+} channels (Corey *et al*. 1984; Szikra *et al*. 2008) to maintain proper basal calcium levels in the soma and terminal regions of rods. Intraterminal calcium levels regulate synaptic release whereas somatic calcium levels are more important for regulating gene expression and other cell functions (Clapham, 2007). Maintaining proper basal calcium levels is critical for photoreceptor cell health since both excessively high (Chang *et al*. 1993; Doonan *et al*. 2005; Hara & Snyder, 2007) and excessively low (Woodruff *et al.* 2003; Fain, 2006) intracellular calcium levels can lead to photoreceptor degeneration.

The sustained depolarization of rods in darkness promotes the release of Ca^{2+} from intracellular stores (Krizaj *et al*. 1999, 2003; Suryanarayanan & Slaughter, 2006; Cadetti *et al*. 2006). If not replenished, ER stores near the rod terminal would soon be emptied of Ca^{2+} in darkness. Frog rods possess a continuous network of smooth ER extending from the synaptic terminal to the axon hillock (Mercurio & Holtzman, 1982). Release of Ca^{2+}, and thus depletion of stores, by CICR will occur preferentially near the base of the terminal where Ca^{2+} channels are clustered (Nachman-Clewner *et al.* 1999; Cadetti *et al.* 2006), but replenishment of Ca^{2+} stores is likely to involve the entire ER network. Ca^{2+} exiting the ER at the base of the terminal could thus be replaced by Ca^{2+} ions diffusing within the ER from more distant parts of the cell where release from stores is minimal. The balance between localized release and global replenishment throughout the entire ER network could allow the ER to funnel Ca^{2+} from more distant parts of the cell to cytoplasm near the ribbon. Supplementing Ca^{2+} entering through voltage-gated Ca^{2+} channels by CICR may help to sustain release in darkness since maintained depolarization at the dark resting membrane potential can inhibit I_{Ca} by >50% (Rabl & Thoreson, 2002). In addition to helping maintain synaptic release rates in darkness, the increase in intraterminal Ca^{2+} accompanying CICR may enhance the likelihood of simultaneous vesicle fusion events (Suryanarayanan & Slaughter, 2006). Rods are capable of responding to single photons of light (Baylor *et al.* 1979) and small single photon responses are transmitted with good reliability to second order neurons (Field *et al.* 2005). By increasing release rates and the likelihood of simultaneous fusion events, CICR may improve the signal to noise ratio in the post-synaptic detection of changes in release and thereby help detect small luminance changes.

Acknowledgments

Supported by NIH grants EY10542 (WBT) and EY014700 (CWM), as well as Research to Prevent Blindness. The authors thank Dr. Keshore Bidasee for generously providing ryanodine.

Abbreviations

CICR	calcium-induced calcium release
ER	endoplasmic reticulum
OPL	outer plexiform layer
RBC	rod bipolar cells
SERCA2	Sarco/Endoplasmic Reticulum Ca^{2+}-ATPase, CPPG, (RS)-a-cyclopropyl-4-phosphonophenylglycine
L-AP4	L- (+) - 2-amino-4-phosphonobutyric acid

REFERENCES

Babai N, Thoreson WB. Horizontal cell feedback regulates calcium currents and intracellular calcium levels in rod photoreceptors of salamander and mouse retina. J Physiol (Lond) 2009;587:2353–2364. [PubMed: 19332495]

Barnes S, Deschenes MC. Contribution of Ca and Ca-activated Cl channels to regenerative depolarization and membrane bistability of cone photoreceptors. J Neurophyiol 1992;68:745–755.

Barnes S, Hille B. Ionic channels of the inner segment of tiger salamander cone photoreceptors. J Gen Physiol 1989;94:719–743. [PubMed: 2482325]

Baumann L, Gerstner A, Zong X, Biel M, Wahl-Schott C. Functional characterization of the L-type Ca^{2+} channel Cav1.4α1 from mouse retina. Invest Ophthalmol Vis Sci 2004;45:708–713. [PubMed: 14744918]

Baylor DA, Lamb TD, Yau K-W. Responses of retinal rods to single photons. J Physiol (Lond) 1979;288:613–634. [PubMed: 112243]

Bouchard R, Pattarini R, Geiger JD. Presence and functional significance of presynaptic ryanodine receptors. Prog Neurobiol 2003;69:391–418. [PubMed: 12880633]

Bui BV, Fortune B. Ganglion cell contributions to the rat full-field electroretinogram. J Physiol (Lond) 2004;15:153–173. [PubMed: 14578484]

Burkhardt DA, Gottesman J, Thoreson WB. Prolonged depolarization in turtle cones evoked by current injection and stimulation of the receptive field surround. J Physiol (Lond) 1988;407:329–348. [PubMed: 3256619]

Burkhardt DA, Zhang SQ, Gottesman J. Prolonged depolarization in rods in situ. Vis Neurosci 1991;6:607–614. [PubMed: 1909172]

Cadetti L, Bryson EJ, Ciccone CA, Rabl K, Thoreson WB. Calcium-induced calcium release in rod photoreceptor terminals boosts synaptic transmission during maintained depolarization. Eur J Neurosci 2006;23:2983–2990. [PubMed: 16819987]

Capovilla M, Cervetto L, Torre V. Antagonism between steady light and phosphodiesterase inhibitors on the kinetics of rod photoresponses. Proc Natl Acad Sci U S A 1982;79:6698–6702. [PubMed: 6183667]

Chang GQ, Hao Y, Wong F. Apoptosis: final common pathway of photoreceptor death in rd, rds, and rhodopsin mutant mice. Neuron 1993;11:595–605. [PubMed: 8398150]

Clapham DE. Calcium signaling. Cell 2007;131:1047–1058. [PubMed: 18083096]

Collin T, Marty A, Llano I. Presynaptic calcium stores and synaptic transmission. Curr Opin Neurobiol 2005;15:275–81. [PubMed: 15919193]

Corey DP, Dubinsky JM, Schwartz EA. The calcium current in inner segments of rods from the salamander (*Ambystoma tigrinum*) retina. J Physiol (Lond) 1984;354:557–575. [PubMed: 6090654]

Doonan F, Donovan M, Cotter TG. Activation of multiple pathways during photoreceptor apoptosis in the rd mouse. Invest Ophthalmol Vis Sci 2005;46:3530–3538. [PubMed: 16186330]

Fain GL. Why photoreceptors die (and why they don't). Bioessays 2006;28:344–354. [PubMed: 16547945]

Field GD, Sampath AP, Rieke F. Retinal processing near absolute threshold: from behavior to mechanism. Annu Rev Physiol 2005;67:491–514. [PubMed: 15709967]

Hara MR, Snyder SH. Cell signaling and neuronal death. Annu Rev Pharmacol Toxicol 2007;47:117–141. [PubMed: 16879082]

Hasegawa J, Obara T, Tanaka K, Tachibana M. High-density presynaptic transporters are required for glutamate removal from the first visual synapse. Neuron 2006;50:63–74. [PubMed: 16600856]

Heidelberger R, Thoreson WB, Witkovsky P. Synaptic transmission at retinal ribbon synapses. Prog Retin Eye Res 2005;24:682–720. [PubMed: 16027025]

Koschak A, Reimer D, Walter D, Hoda J-C, Heinzle T, Grabner M, Striessnig J. Cav1.4α1 subunits can form slowly inactivating dihydropyridine-sensitive L-type Ca^{2+} channels lacking Ca^{2+}-dependent inactivation. J Neurosci 2003;23:6041–6049. [PubMed: 12853422]

Krizaj D, Bao JX, Schmitz Y, Witkovsky P, Copenhagen DR. Caffeine-sensitive calcium stores regulate synaptic transmission from retinal rod photoreceptors. J Neurosci 1999;19:7249–7261. [PubMed: 10460231]

Krizaj D, Lai FA, Copenhagen DR. Ryanodine stores and calcium regulation in the inner segments of salamander rods and cones. J Physiol (Lond) 2003;547:761–774. [PubMed: 12562925]

Lelli A, Perin P, Martini M, Ciubotaru CD, Prigioni I, Valli P, Rossi ML, Mammano F. Presynaptic calcium stores modulate afferent release in vestibular hair cells. J Neurosci 2003;23:6894–6903. [PubMed: 12890784]

McRory JE, Hamid J, Doering CJ, Garcia E, Parker R, Hamming, Chen L, Hildebrand M, Beedle AM, Feldcamp L, Zamponi GW, Snutch TP. The CACNA1F gene encodes an L-type calcium channel with unique biophysical properties and tissue distribution. J Neurosci 2004;24:1707–1718. [PubMed: 14973233]

Mercurio AM, Holtzman E. Smooth endoplasmic reticulum and other agranular reticulum in frog retinal photoreceptors. J Neurocytol 1982;11:263–293. [PubMed: 6978386]

Nachman-Clewner M, Jules R, Townes-Anderson E. L-type calcium channels in the photoreceptor ribbon synapse: localization and role in plasticity. J Comp Neurol 1999;415:1–16. [PubMed: 10540354]

Nakatani K, Tamura T, K.W. Yau KW. Light adaptation in retinal rods of the rabbit and two other nonprimate mammals. J Gen Physiol 1991;97:413–435. [PubMed: 2037836]

Nawy S. Desensitization of the mGluR6 transduction current in tiger salamander On bipolar cells. J Physiol 2004;558:137–146. [PubMed: 15146044]

Newman EA, Bartosch R. An eyecup preparation for the rat and mouse. J Neurosci Methods 1999;93:169–175. [PubMed: 10634502]

Nikonov SS, Kholodenko R, Lem J, Pugh EN Jr. Physiological features of the S- and M-cone photoreceptors of wild-type mice from single-cell recordings. J Gen Physiol 2006;127:359–374. [PubMed: 16567464]

Pessah IN, Zimanyi I. Characterization of multiple [3H]ryanodine binding sites on the Ca^{2+} release channel of sarcoplasmic reticulum from skeletal and cardiac muscle: evidence for a sequential mechanism in ryanodine action. Mol Pharmacol 1991;39:679–689. [PubMed: 1851961]

Rabl K, Thoreson WB. Calcium-dependent inactivation and depletion of synaptic cleft calcium ions combine to regulate rod calcium currents under physiological conditions. Eur J Neurosci 2002;16:2070–2077. [PubMed: 12473074]

Robson JG, Frishman LJ. Dissecting the dark-adapted electroretinogram. Doc Ophthalmol 1998;95:187–215. [PubMed: 10532405]

Rousseau E, Smith JS, Meissner G. Ryanodine modifies conductance and gating behavior of single Ca^{2+} release channel. Am J Physiol 1987;253:C364–C368. [PubMed: 2443015]

Schneider T, Zrenner E. The influence of phosphodiesterase inhibitors on ERG and optic nerve response of the cat. Invest Ophthalmol Vis Sci 1986;27:1395–1403. [PubMed: 3744729]

Sharma S, Ball SL, Peachey NS. Pharmacological studies of the mouse cone electroretinogram. Vis Neurosci 2005;22:631–636. [PubMed: 16332274]

Shoshan-Barmatz V, Orr I, Martin C, Vardi N. Novel ryanodine-binding properties in mammalian retina. Int J Biochem Cell Biol 2005;37:1681–1695. [PubMed: 15896674]

Shoshan-Barmatz V, Zakar M, Shmuelivich F, Nahon E, Vardi N. Retina expresses a novel variant of the ryanodine receptor. Eur J Neurosci 2007;26:3113–3125. [PubMed: 18005065]

Suryanarayanan A, Slaughter MM. Synaptic transmission mediated by internal calcium stores in rod photoreceptors. J Neurosci 2006;26:1759–1766. [PubMed: 16467524]

Stockton RA, Slaughter MM. B-wave of the electroretinogram. A reflection of ON bipolar cell activity. J Gen Physiol 1989;93:101–122. [PubMed: 2915211]

Szikra T, Cusato K, Thoreson WB, Barabas P, Bartoletti TM, Krizaj D. Depletion of calcium stores regulates calcium influx and signal transmission in rod photoreceptors. J Physiol (Lond) 2008;586:4859–4875. [PubMed: 18755743]

Thoreson WB, Burkhardt DA. Ionic influences on the prolonged depolarization of turtle cones *in situ*. J. Neurophysiol 1991;65:96–110. [PubMed: 1900325]

Thoreson WB, Witkovsky P. Glutamate receptors and circuits in the vertebrate retina. Prog Ret Eye Res 1999;18:765–810.

Thoreson WB, Stella SL Jr, Bryson EI, Clements J, Witkovsky P. D2-like dopamine receptors promote interactions between calcium and chloride channels that diminish rod synaptic transfer in the salamander retina. Vis Neurosci 2002;19:235–247. [PubMed: 12392173]

Ungar F, Piscopo I, Holtzman E. Calcium accumulation in intracellular compartments of frog retinal rod photoreceptors. Brain Res 1981;205:200–206. [PubMed: 6970606]

Woodruff ML, Wang Z, Chung HY, Redmond TM, Fain GL, Lem J. Spontaneous activity of opsin apoprotein is a cause of Leber congenital amaurosis. Nat Genet 2003;35:158–164. [PubMed: 14517541]

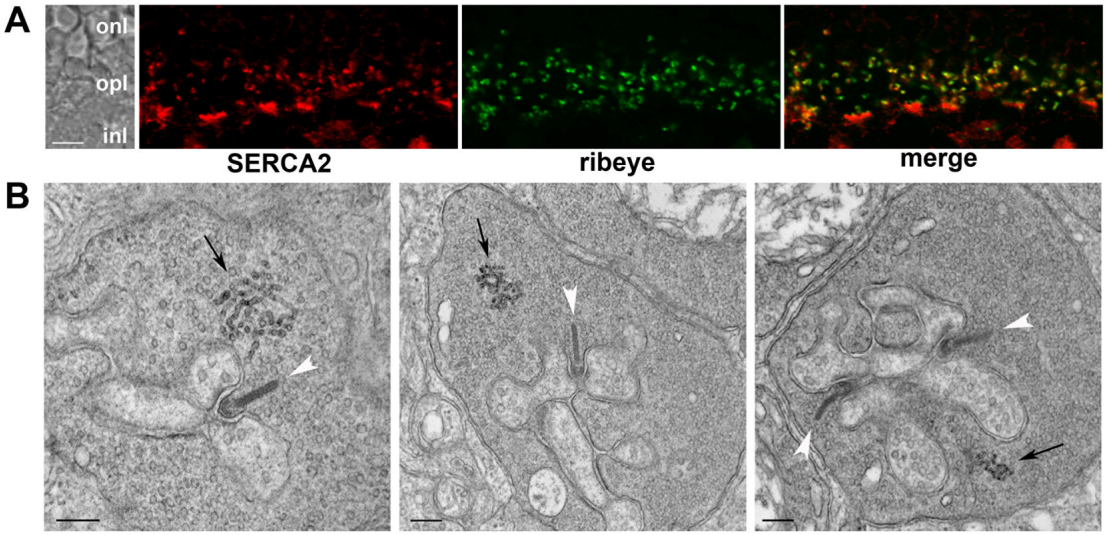

Figure 1. Rod terminals in the mouse retina contain an ER-like structure

A. Confocal image showing an optical section of the mouse OPL double labeled for SERCA2 (red) and the synaptic ribbon protein, ribeye (green). In the merged image (right panel) areas of overlap appear yellow. B. Electron micrographs of mouse rod terminals. Synaptic ribbons are indicated with white arrowheads and putative ER with black arrows. The scale bars represent 5 μm in A and 200 nm in B. Abbreviations: onl, outer nuclear layer; opl, outer plexiform layer; inl, inner nuclear layer.

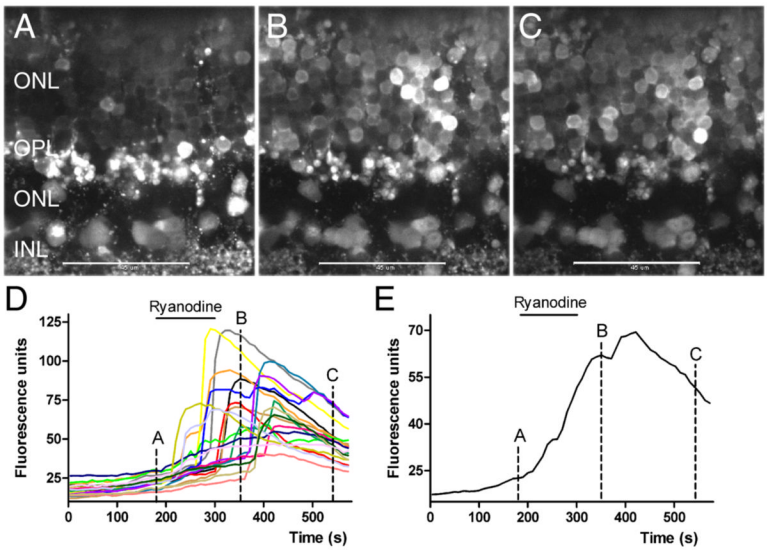

Fig. 2. Stimulating CICR with 10 μM ryanodine evoked Ca^{2+} increases in mouse rod somas

A-C. Outer nuclear layer of the mouse retina loaded with the Ca^{2+}-sensitive dye, Fluo4-AM, in control conditions (A), in the presence of ryanodine (10 μM, B) and during washout of ryanodine (C). Images show single confocal sections. D. Fluo4 fluorescence changes measured in 19 different rod somas. E. Average Fluo4 fluorescence change in these somas. Images in A-C were obtained at the time points indicated in the graphs. Bar: 10 μm.

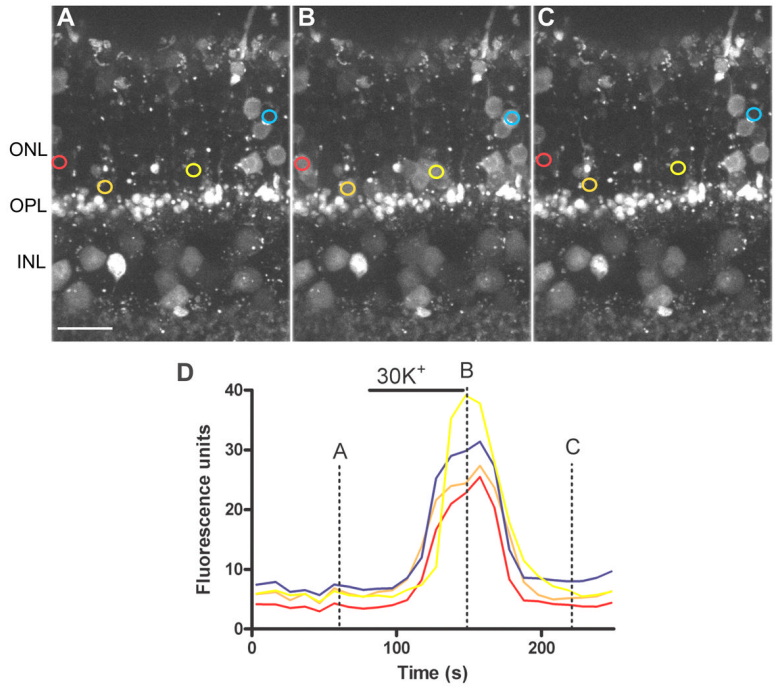

Fig. 3. Depolarizing rods with 30 mM KCl evoked rapid Ca^{2+} increases

Outer mouse retina loaded with the Ca^{2+}-sensitive dye, Fluo4-AM, in control conditions (A), in the presence of high K^+ and following washout (C). Images are stacks of 5 confocal sections obtained at 1 μm intervals. D. Fluo4 fluorescence changes measured in different rod somas. The traces in D and corresponding regions of interest in panels A-C are shown in the same color. Bar: 10 μm.

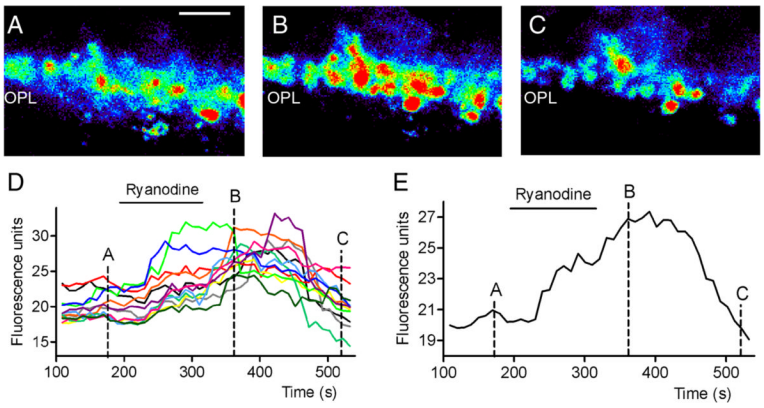

Fig. 4. Ca^{2+} increases in rod terminals evoked by stimulation of CICR with 10 μM ryanodine

Pseudocolor images of a single confocal section of the outer plexiform layer loaded with Fluo4 in control conditions (A), after bath application of 10 μM ryanodine (B), and following washout (C). Bar: 10 μm. D. Fluo4 fluorescence changes measured from 12 terminals at 10 s interval. E. Average Fluo4 fluorescence changes from the same terminals. Images in A-C were obtained at the time points indicated in the graphs.

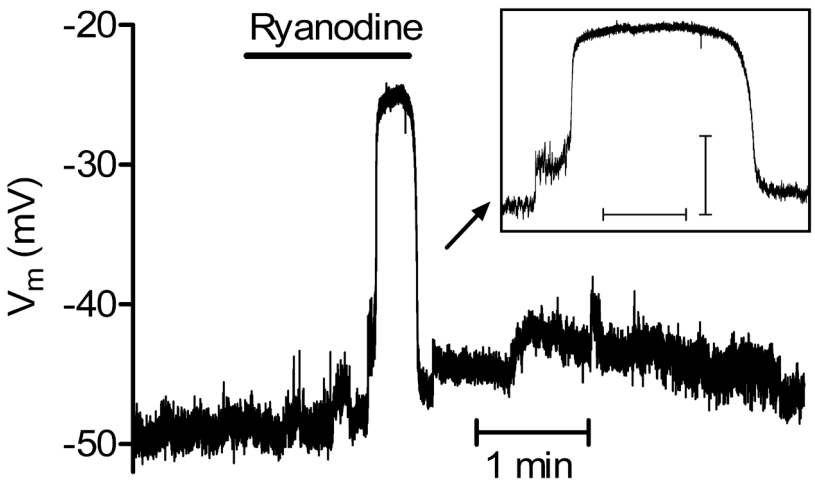

Fig. 5. Activating CICR with a low concentration of ryanodine (10 μM) depolarized rods

In addition to a modest initial depolarization, a large, prolonged depolarizing response was also sometimes observed in some cells. The prolonged depolarizing response is expanded in the inset. Scale bars for inset: abscissa, 10 s; ordinate, 10 mV.

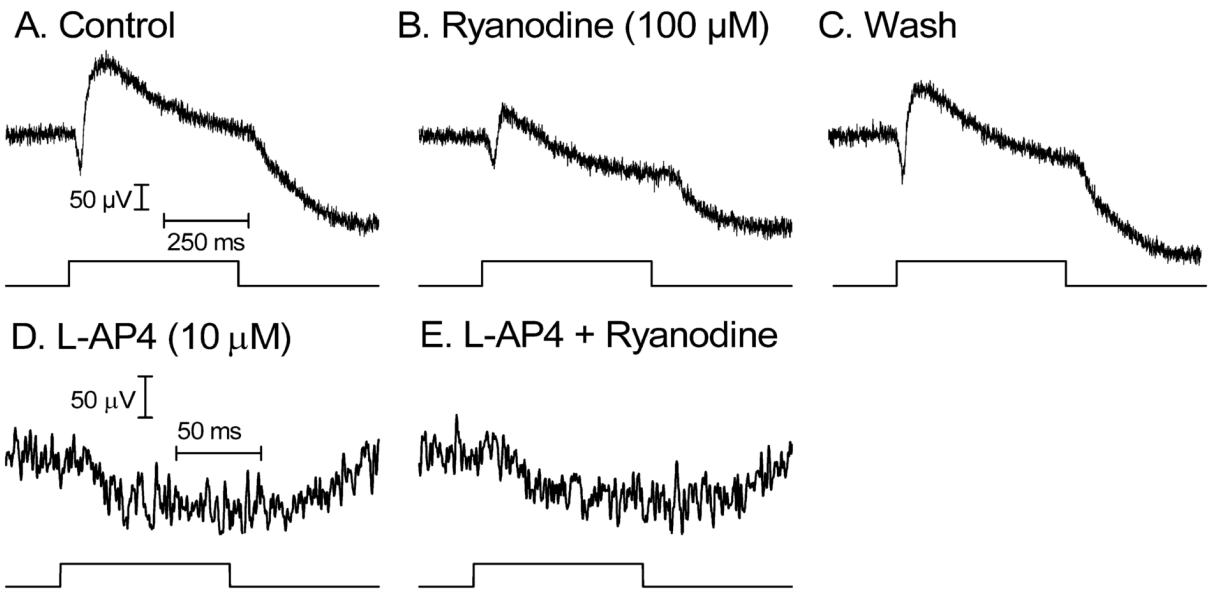

Fig. 6. Inhibiting CICR with a high concentration of ryanodine (100 μM) reduced the ERG b-wave but not a-wave indicating a reduction in synaptic transmission from rods

A. Intraretinal ERG evoked by 0.5 s light flash and recorded in control conditions. B. ERG after ryanodine was bath applied for 3 min. C. ERG recovered after washout. Light intensity: 4×10^3 480 nm equivalent photons/s/μm^2. D. A-wave recorded after blocking the ERG b-wave with bath applied L-AP4 (10 μM). The light stimulus in this experiment was 100 ms flash of 1.8×10^4 480 nm equivalent photons/s/μm^2. E. AP4-isolated a-wave after application of ryanodine (100 μM).

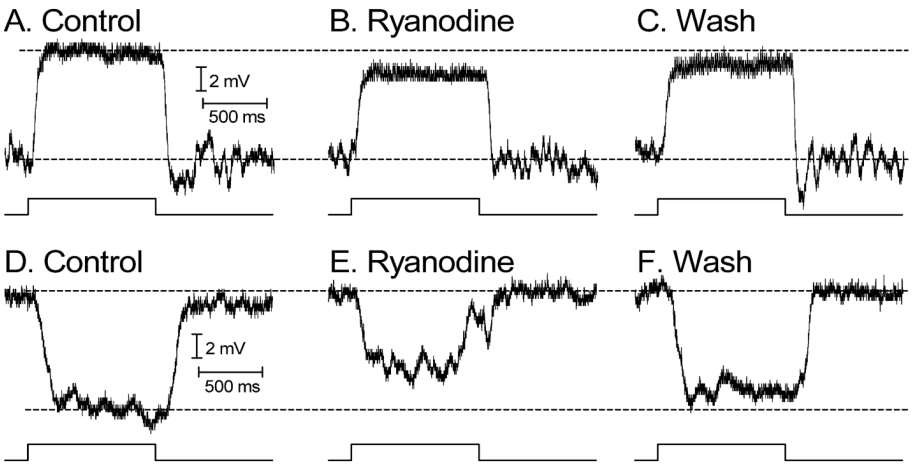

Fig. 7. Ryanodine (100 μM) inhibited depolarizing light responses of RBCs and hyperpolarizing light responses of presumptive horizontal cells

Light-evoked voltage responses were recorded from mouse retinal slices using perforated patch recording techniques. A. Response of an RBC in control conditions evoked by a saturating light flash. B. Light response of the same cell recorded in the presence of ryanodine. C. Response recorded following washout. Intensity: 4×10^3 480 nm equivalent photons/s/μm^2. D. Response of a presumptive horizontal cell in control conditions evoked by a bright saturating light flash. E. Light response of the same cell recorded in the presence of ryanodine. F. Response recorded following washout. Dark membrane potentials were aligned in the illustration. Intensity: 1.8×10^4 480 nm equivalent photons/s/μm^2.

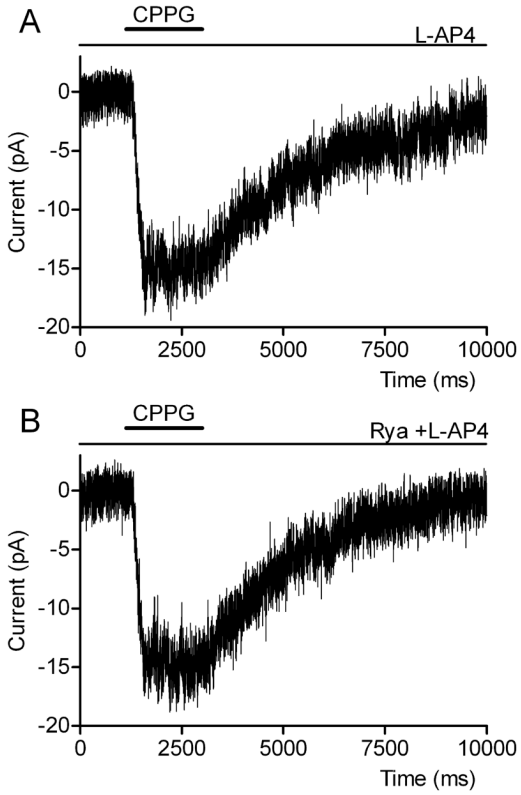

Fig. 8. Ryanodine (100 μM) did not alter mGluR6-mediated post-synaptic responses of voltage-clamped RBCs

A. Inward current generated by puffing CPPG (600 μM) into the OPL while continuously superfusing L-AP4 (4 μM). B. CPPG applied in the presence of L-AP4 and ryanodine (100 μM).

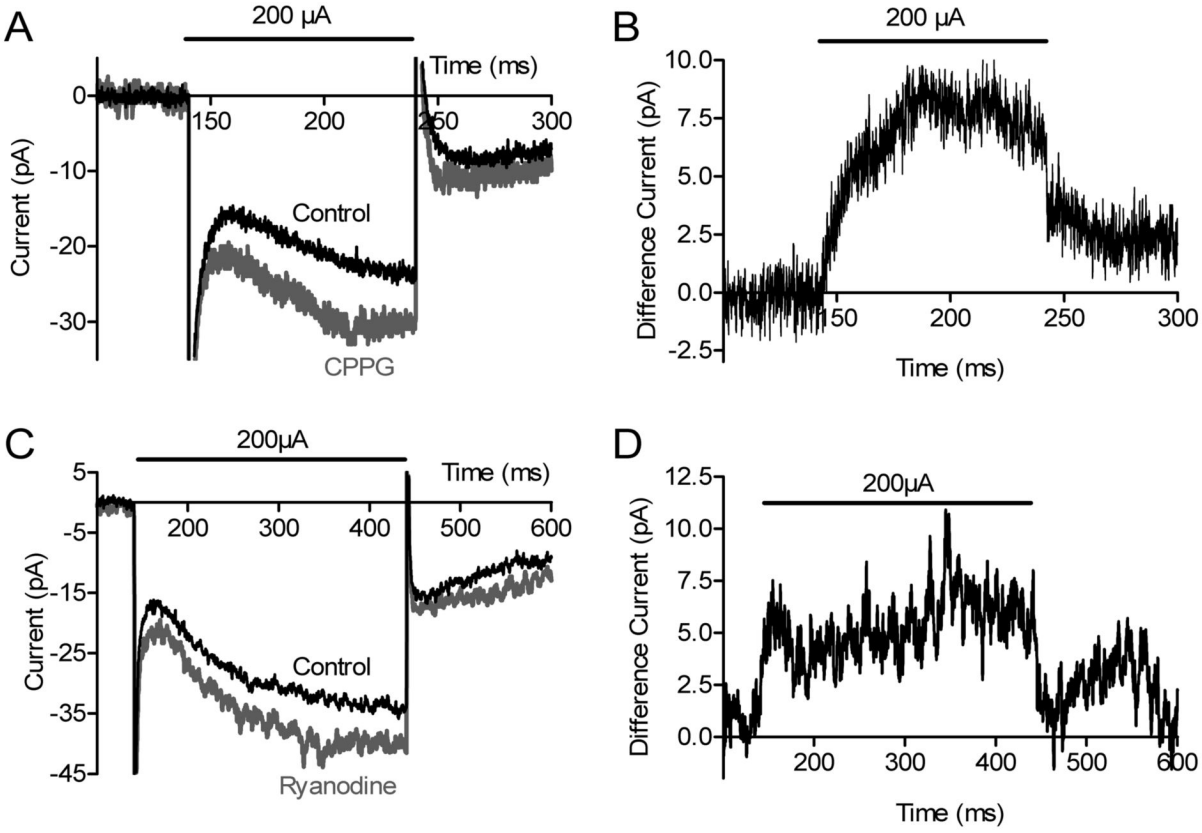

Fig. 9. Ryanodine (100 µM) inhibited outward glutamatergic currents evoked by current pulses injected into the outer segment layer

Current injection stimulated currents in RBCs consisting of both direct inward currents and glutamatergic outward currents. Glutamatergic outward currents were blocked by the mGluR6 antagonist CPPG (600 µM) (A). The mGluR6-mediated outward current can be seen more clearly by subtracting the control response from the response observed after application of CPPG (B). Like CPPG, ryanodine (100 µM) inhibited outward currents in RBCs evoked by electrical stimulation of rods (C). D shows the difference current obtained by subtracting the control response from the response obtained after application of ryanodine (100 µM).